The Modeling and Design of An Index Finger Rehabilitation Exoskeleton with High Suitability

Rui Qian [1, †], Chengmin Yu [2, †] and Taihong Zhang [3, †, *]

[1] Hongwen School, Qingdao, China

[2] Department of automation, Nanjing University of Aeronautics and Astronautics, Nanjing, China

[3] School of mechanical engineering, Donghua University, Shanghai, China

* Corresponding author Email: 190820224@mail.dhu.edu.cn

† These authors are equal contribution

Abstract. With the increasing demand of hand rehabilitation training, people pay more attention to the hand exoskeleton machine. In contrast to this growing demand, most exoskeletons have a weak adaptability, meaning that almost every exoskeleton is tailored to the patient's individual hand data. Through calculation, modeling, and simulation experiments, this paper aims to add additional sensors to the MCP and PIP joints to obtain more accurate data, and further increase joint mobility, flexibility, and adaptability based on the adjustable pulley to achieve better rehabilitation results and lower cost. Based on the existing underactuated exoskeleton, this work has added sensors, sliding contact modules and retractable link rods at the nodes between the MCP and PIP joints to improve the accuracy and adaptability of the exoskeleton.

Keywords: Hand Exoskeleton; Efficient Rehabilitation; Underactuated Driven; Redundant Sensor.

1. Introduction

In 2050, the world's population of people who are aged 60 and above will exceed 2 billion [1], and the consequent problems will also have certain impacts on the society. The aging of the physical body is an obstacle to the normal life of the elderly population. The loosening of muscle tissues, the decline of reaction ability and the damage of coordination and organization ability brought about by aging will inevitably make the daily life of the elderly more difficult [2]. At the same time, the probability of stroke is also gradually increasing, casting a shadow on the normal life of the elderly people. According to the China Cardiovascular Health and Disease Report, the number of stroke patients in China will reach 267 million in 2022, accounting for 1.85 percent of the population. Among patients, the increase was most pronounced in the older group over 65 years of age. As the proportion of aging population increases, the number of stroke patients also increases, and the incidence rate further increases [3]. Stroke has the characteristics of high incidence and disability rate, and the hemiplegia and numbness caused by it also brings detrimental effects to patients [4].

Although the problems mentioned above have caused many impacts on individuals and society, the corresponding stroke rehabilitation process is one of the most widely used method to lower the disability rate [4]. Due to the fundamental position of hand for maneuvering operation in daily life, the rehabilitation training of hand muscles has significant effects and irreplaceable significance for the for-stroke patients to recover from sequela. Hand rehabilitation training has the characteristics of high cost, high difficulty and high time consumption. Paradoxically, there is a huge gap between the number of patients and the number of rehabilitation physicians, resulting in a situation of more patients and fewer physicians. Therefore, under the background of the excellent assisting ability of mechanical exoskeleton in helping to promote muscle recovery training, hand rehabilitation robot has become an important research topic.

The hand exoskeleton has become much more mature than the preliminary conception and research with the development of technology innovations. From the end contact type in the early 21st century to the currently widely used exoskeleton type, the hand rehabilitation robot has undergone many generations of improvements, and derived different kinds of robotic exoskeletons each with unique advantages and disadvantages. But no matter what kind of mechanical exoskeleton they apply, they all will face a common problem: the adaptation of the mechanical exoskeleton. Since hand exoskeleton requires to highly match with the finger joints, the fixed size exoskeleton cannot adapt to all the hand types. As a result, low adaptability makes customized exoskeletons a common phenomenon. Therefore, the cost of production is greatly driven up as mass production of the exoskeleton is not able to realize.

Correct geometric parameters, which depends on the relative attachment of the exoskeleton to the hand, is crucial for the controller's function. In addition, measuring the exact geometric parameters depending on the wearer's hand is difficult to achieve because the exact position of the finger joint axis is difficult to determine. To solve these problems, this work added two additional sensors to the underactuated exoskeleton with adjustable sliders to estimate uncertain geometric parameters, thereby enhancing the control of MCP and PIP joint adaptability and flexibility.

Next, this work will introduce the design and control of our index finger exoskeleton. Experiments on the patterns of the movement of the finger show that the index finger joint has two movement modes: flexion and extension and abduction-adduction. However, the abduction-adduction movement has little influence on the normal function of the index finger [5]. Considering the complexity of the design and the cost of the equipment, this work did not consider this type of movement of the index finger. At the same time, medically, since the PIP joint and DIP joint of the index finger are coupled [6], this work does not provide active control of the DIP joint, and only use Bowden cable to drive the MCP and PIP joints. In order improve the adaptability of the index finger exoskeleton, this work carried out the adjustable design of MCP and PIP, which are two important motor closed chain connecting rods, including the mechanical design of the adjustable unit.

In order to make this medical index finger exoskeleton achieve the task of helping patients actively complete the recovery trajectory, this work adopted a more effective force control strategy rather than position control strategy [7, 8]. However, the force control strategy also requires the precise control of torque. As a result, the idea of using a Bowden cable-based series elastic actuator (SEA) as the driving unit and spring deformation to achieve precise torque control was applied in the exoskeleton [9]. When the exoskeleton is worn on the fingers of different patients, the joint axis is difficult to determine and the geometric parameters are changed [10]. Therefore, it is very important to estimate the geometric parameters. To achieve this goal, this work considered adding redundant sensors near the MCP and PIP joints, which could help us determine geometric parameters to enhance the suitability of the exoskeleton to the index finger of different patients.

With this exoskeleton design, this work hopes to achieve the following goals: First, to ensure proper movement of the forefinger, ensure the comfortableness of interaction, and avoid joint dislocation. Next, the exoskeleton is expected to achieve precise torque control. Third, be able guide patients to complete the training routes of the exoskeleton. Fourth, to fit through different patients on mechanical structure and movement. Lastly, to have a smaller sized scale and less cost of production.

2. Method

The movement of the index finger is divided into two types, namely flexion and extension and abduction-adduction. Structurally, the index finger is divided into the proximal metacarpophalangeal joint (MCP) (PIP) and distal (DIP). The MCP exhibits abduction-adduction and flexion and extension movements while the PIP and DIP only exhibit flexion and extension movements. Moreover, the use of invasion-adduction in general finger movement is not very common. However, in the exoskeleton design process, the integration of abduction and adduction motion into the design will increase the number of degrees of freedom of the mechanism and make the design elements extremely complex, so this work will not consider the abduction and adduction motion in the exoskeleton design.

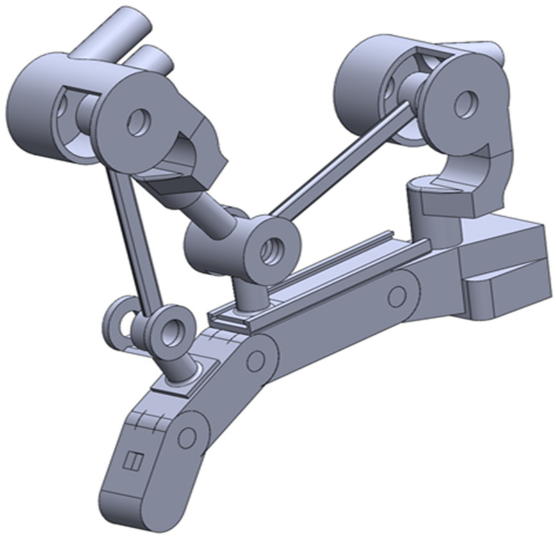

Fig 1. The Solidworks model of the designed index finger exoskeleton

2.1 Kinematic Designs

To reduce the harmful force between the index finger exoskeleton and the index finger, avoiding joint dislocation is a very important point in the design process of the exoskeleton. Considering the comfort of wearing and the flexibility of movement, this work has installed a slider on a movement chain parallel to the finger. During movement, the slider will automatically fit into place, ensuring that the force is perpendicular to the finger downwards. The design also gives the index finger exoskeleton a better suitability. Medically, the DIP and PIP joints of the index finger are coupled, so no active control is provided for the DIP joints. Instead, the MCP and PIP joints are driven by a series elastic device based on Bowden cables, which can transmit the amount of force through a spring. In this way, precise torque control is achieved. To solve the problem, this work decided to reduce the degrees of freedom and remove the slider of the PIP joint (Fig. 1). But such a design will inevitably bring about the problem of larger harmful component.

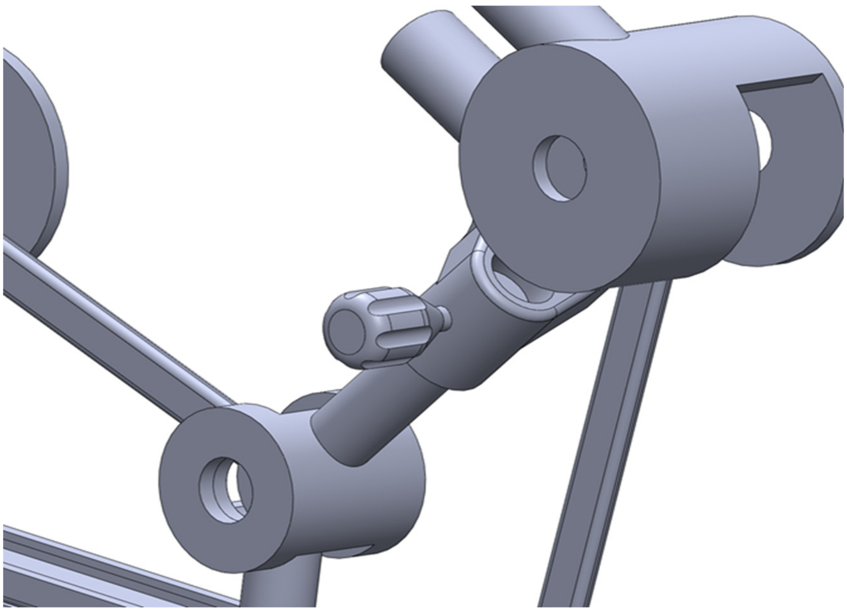

Fig 2. The adjustable connecting rod between MCP and PIP joints

2.2 Size Adaptability

Because of the MCP joint of the index finger, most of the index finger exoskeletons are difficult to reproduce the flexibility and omni directivity of index finger movement. At the same time, the same type of exoskeleton cannot fit all hand types, and the adaptation of exoskeleton joints is affected with the change of hand types. This also makes the design of the index finger exoskeleton extra difficult. In response, this work used a sliding bar instead of a fixed bar between the MCP and PIP joints to cope with finger length variations (Fig. 2) [11].

2.3 Model

In this model, the work uses the five rotational joints, and two sliding joints, respectively between the PIP and DIP joints and MCP and PIP joints. The whole device is strapped to the hand and secured with Velcro at four points attached to the finger. The slide bar made suitable for finger size is fixed with screws. If the finger size is different, the screw will be loosened, the slider to cancel the lock, then you can adjust the length.

2.4 Redundant Sensors

It is undeniable that the use of pulleys brings more complex movement trajectory to the whole system, which poses a great challenge to the programming of machine movement behavior. When the exoskeleton length changes, geometric parameters is difficult to determine. In order to cope with the uncertainty and collect more detailed data to support the mechanical behavior of algorithm to improve the mechanical adaptability, this work each added redundant sensors to the nodes of the joint of MCP and PIP to collect data to ensure that the exoskeleton can move smoothly and comfortably.

In order to ensure the flexibility and adaptability of the index finger joint, this work need to know the flexibility angle of each joint of the index finger and the average length of each finger block to meet the needs of different hand shapes as much as possible.

2.5 Kinematic Modelling

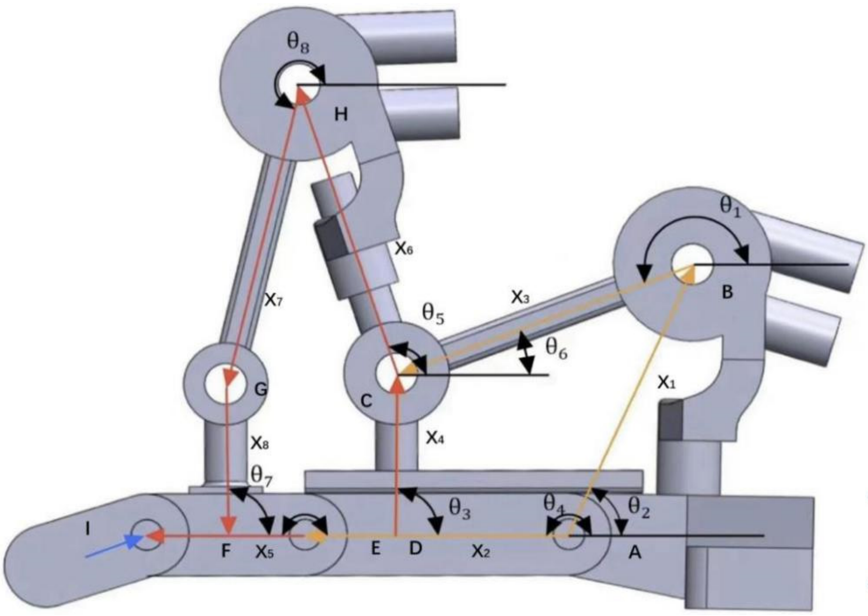

Fig 3. The labelling of the kinematic model

As we can see in the figure, the range of motion of MP and PIP joints has a significant impact on the posture and motion of the entire exoskeleton system. The aggregated data are shown in the following table [12]:

Table 1. The range of movement of the joints

Joint	Range of movement (°)
MCP (forward bending)	90
MCP (backward bending)	30
PIP (forward bending)	90
DIP (forward bending)	60

Based on the data above, this work can determine the relative expansion adjustment ratio of exoskeleton's extendable rod length and optimize the motion mode of underactuation control through the range of motion of each joint.

As can be seen from the table above, the two joints to which the D-finger block is attached have a great range of motion. Improved control of the D-finger block has significant implications for overall braking. Therefore, the slidable contactability module and the retractable link lever are extended on the most critical C-block. Prior to actuation, the retractable link bar will be adjusted to the bar length based on the input of actual measured proportional data for each finger. During motion, nodes B and G move the slidable contactability module of the D finger block back and forth on the slide while the Bowden line is rotated for underactuation-based control.

Since the DIP and PIP joints of the index finger are coupled, the modeling was performed only for the position and kinematics of the closed chain formed by the index finger and the exoskeleton at the PIP and MCP joints of this exoskeleton (Fig. 3). Here, by analyzing the geometric features of the closed chain 1 (see Fig. 3 orange) and closed chain 2 (see Fig. 3 red), this work solved the forward and reverse kinematics of this index finger exoskeleton.

The geometric relations of the closed chain 1 can be described by the vectors AB, BC, AD, DC (1).

$$AB + BC = AD + DC$$
$$x_1 e^{i\theta_2} + x_3 e^{i\theta_1} = x_2 e^{i\theta_4} + x_4 e^{i\theta_3} \tag{1}$$

In this case $\theta_3 = \theta_4 - \frac{\pi}{2}$. In this equation, since x_2 depends on the length of the wearer's knuckles, x_2 is eliminated in the calculation, and (2) can be found when the closed chain 1 is in forward motion.

$$X\tan^2\theta_4/2 + Y\tan\theta_4/2 + K = 0 \tag{2}$$

Of which

$$X = x_1 \sin\theta_2 + x_3 \sin\theta_1 - x_4$$
$$Y = 2x_1 \cos\theta_2 + 2x_3 \cos\theta_1$$
$$K = -x_1 \sin\theta_2 - x_3 \sin\theta_1 - x_4$$

In reverse motion there is (3)

$$X\tan^2\theta_1/2 + Y\tan\theta_1 \tag{3}$$

Of which

$$X = x_1 \sin(\theta_4 - \theta_2) - x_3 \sin\theta_4 - x_4$$
$$Y = -2x_3 \cos\theta_4$$
$$K = x_1 \sin(\theta_4 - \theta_2) + x_3 \sin\theta_4 - x_4$$

The forward and reverse motion equations can be derived respectively by combining the forward and reverse motion equations and deriving the derivatives, which are given by (4) and (5).

$$\omega_4 = \frac{x_3 \cos(\theta_4 - \theta_1)}{x_1 \cos(\theta_4 - \theta_2) + x_3 \cos(\theta_4 - \theta_1)} \times \omega_1 \tag{4}$$

$$\omega_1 = \frac{x_1 \cos(\theta_4 - \theta_2) + x_3 \cos(\theta_4 - \theta_1)}{x_3 \cos(\theta_4 - \theta_1)} \times \omega_4 \tag{5}$$

Similarly, the forward and inverse kinematic equations of the exoskeleton and the index finger PIP joint can be obtained by closed chain analysis of closed chain 2, given by (6) and (7).

$$\omega_9 = \frac{X-Y-Z}{X} \times \omega_4 + \frac{Y}{X} \times \omega_5 + \frac{Z}{X} \times \tag{6}$$

$$\omega_8 = \frac{-X+Y+Z}{Z} \times \omega_4 + \frac{X}{Z} \times \omega_5 - \frac{Y}{Z} \times \tag{7}$$

Of which

$$X = x_8 \sin(\theta_4 - \theta_9) - x_5 \cos(\theta_9 - \theta_4)$$
$$Y = x_6 \cos(\theta_5 - \theta_4)$$
$$Z = x_7 \cos(\theta_8 - \theta_4)$$

By relating the kinematic equations of these two joints and differentiating them, this work derived the Jacobi matrix J(θ) for a standard double-link manipulator using the method of J.J. Craig et al [13]

$$v = J(\theta)\dot{\theta}$$

where $[J(\theta)]_{2\times3}$ shows the relationship between finger joint motion and exoskeletal joint motion. This matrix allows to obtain the velocity of translational and vertical motion of each movable joint in plane motion.

$$\begin{bmatrix} \dot{x} \\ \dot{y} \end{bmatrix} = J(\theta) \begin{bmatrix} \dot{\theta}_1 \\ \dot{\theta}_5 \\ \dot{\theta}_8 \end{bmatrix}$$

3. Controls

3.1 Theoretical Derivation

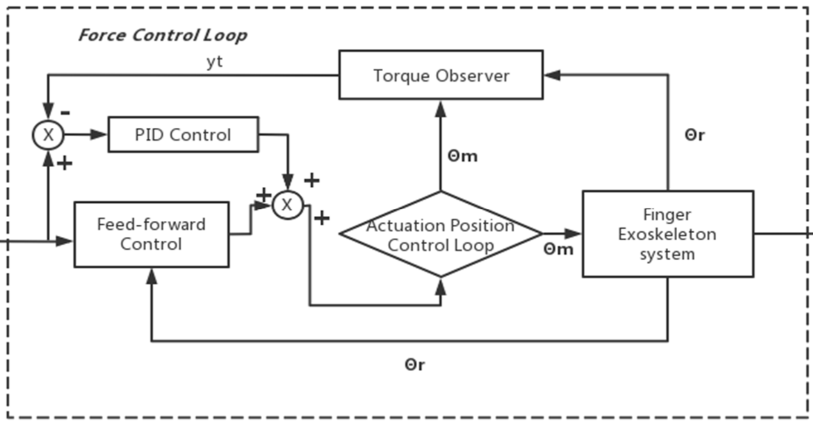

Fig 4. Torque controller structure

Achieving accurate torque control through SEA is a major challenge in the design of this exoskeleton. For the torque involved in the exoskeleton joints as well as the finger joints, this work has designed torque control devices separately (Fig. 4). The role of the exoskeleton joint torque controller is mainly to track the torque trajectory required by the SEA. Equation (8) can be obtained from the way torque transmits force magnitude through spring deformation.

$$\tau_j = (T_2 - T_1)r_j = 2k(r_m\theta_m - r_j(\theta_r - \theta_{r0}))r_j \tag{8}$$

where τ_j is the torque, r_m and r_j are the radius sizes of the pulleys at the drive and joint ends, respectively, and θ_m and θ_r denote the joint angle and motion angle, respectively. From this, the actual output of this torque control system can be obtained and expressed by y_t (9).

$$y_t=[\tau_{j,mcp} \quad \tau_{j,pip}]T=2K(r_m\theta_m - r_j(\theta r - \theta_{r0}))r_j \tag{9}$$

Of which

$$K=\begin{bmatrix} k_{j,mcp} & 0 \\ 0 & k_{j,pip} \end{bmatrix} \qquad \theta_m=\begin{bmatrix} \theta_{m,mcp} \\ \theta_{m,pip} \end{bmatrix} \qquad \theta_r=\begin{bmatrix} \theta_1 \\ \theta_8 \end{bmatrix}$$

K is the matrix representing the magnitude of the effective stiffness of the MCP and PIP joints of the exoskeleton. θ_m is the matrix representing the angles of motion at the drive end, and θ_r is the matrix representing the joint angles of the two drive joints of the exoskeleton. The equation above leads to the PID controller with an attached feedforward controller (10).

$$e_t=y_d-y_t$$

$$u=\frac{1}{r_m}\left(\frac{K^{-1}}{2r_j}y_d + r_j(\theta_r - \theta_{r0})\right) + \mathbf{K}_p\mathbf{e}_t+K_d\dot{\mathbf{e}}_\mathbf{t} + \mathbf{K}_i \int \mathbf{e}_\mathbf{t}dt \tag{10}$$

where e_t is the vector containing the torque error in the PID control, y_d is the torque vector required by the two exoskeleton joints, and u is the input vector of the two exoskeleton joints. The gain matrix of the PID control is as follows

$$\mathbf{K}_p=\begin{bmatrix} k_{p,mcp} & 0 \\ 0 & k_{p,pip} \end{bmatrix} \qquad \mathbf{K}_d=\begin{bmatrix} k_{d,mcp} & 0 \\ 0 & k_{d,pip} \end{bmatrix} \qquad \mathbf{K}_i=\begin{bmatrix} k_{i,mcp} & 0 \\ 0 & k_{i,pip} \end{bmatrix}$$

The principle of the torque controller for the finger joints is basically similar to that of the exoskeleton joints. The role of this controller is to track the magnitude of the torque required on both MCP and PIP finger joints. And since the effect of inertia on this exoskeleton can be neglected [14], the torque of the finger joints (11) can be obtained from the torque of the SEA.

$$y_t=2\mathbf{K}(r_m\theta_m - r_j(\theta_r - \theta_{r0}))r_j \boldsymbol{J}_n^{-T} \tag{11}$$

The Jacobi matrix $\boldsymbol{J}_n$ is used to reflect the relationship between the finger joint torque and the exoskeleton joint torque, which can be obtained by $J(\theta)$, and further deduce the input vector of the PID controller.

It is worth noting that since the position of the finger joint axis is difficult to determine when the human finger is wearing the exoskeleton, this poses difficulty for the four-bar mechanism to obtain the exact Jacobi matrix $J(\theta)$. In this matrix, θ_4, θ_9 is the motion angle of the human finger joints. It is difficult to obtain the magnitude of these two joint angles directly when the axis position is uncertain, so this work used redundant sensors, mainly used to transfer time information, in the two joints of the exoskeleton connected to the MCP and PIP joints. After matching the collected data from one week's tracking of the finger joint rotation with the drive end applied velocity, it is possible to use an optimized technique to estimate uncertain geometric parameters offline. These two redundant sensors weaken the uncertainty of the geometric parameters and the uncertainty of the motion, ensuring that this exoskeleton performs force control in a soothing manner as expected when worn on the index finger of different patients.

4. Results

After the construction of Solidworks model is completed, kinematics analysis is required. This work first built the robot model of the index finger in the MATLAB environment, and then defined the motion of the index finger exoskeleton in reverse so that this work was able to obtain the reasonable motion planning of the index finger exoskeleton.

4.1 The Model of the Index Finger

A model of the human index finger was constructed in the MATLAB environment, and according to the size range of the human finger [15], the distal length of 20, the mid length of 30, and the proximal length 50 were taken to construct the model and verify the motion parameters of this index finger.

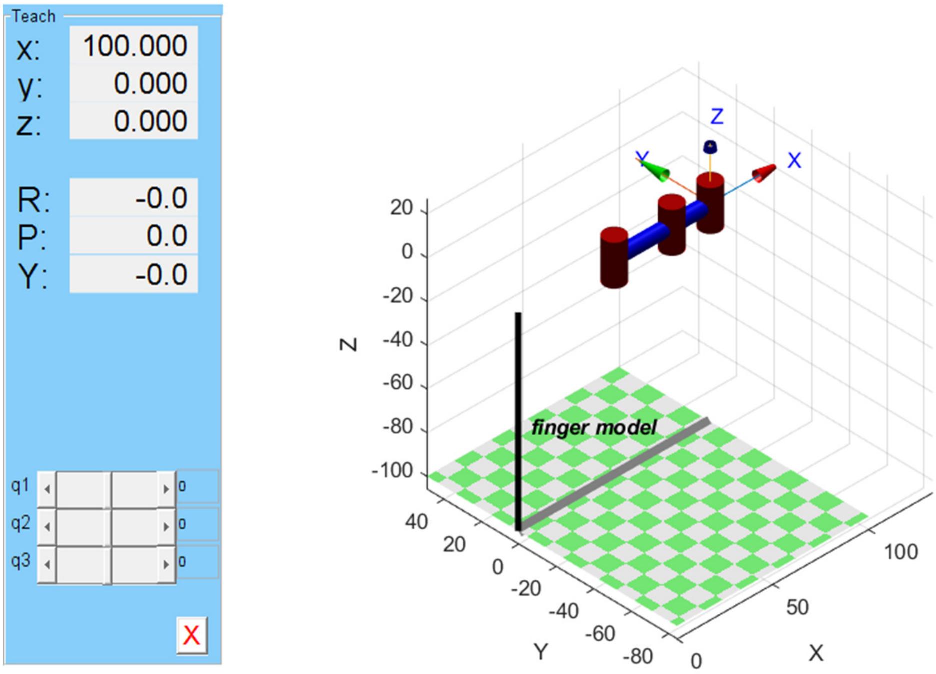

Fig 5. The index finger model constructed in MATLAB environment

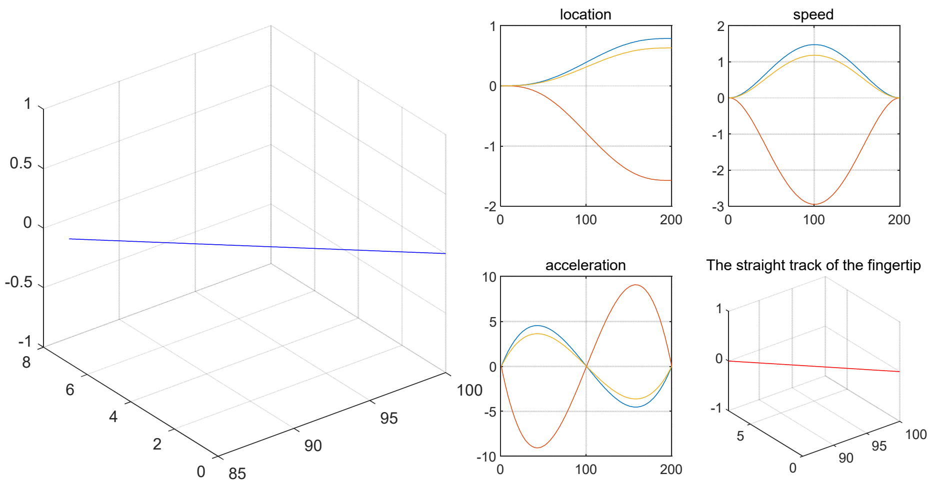

Fig 6. Results of finger kinetics

The displacement, velocity, and acceleration data of the finger motion are specified in MATLAB through the RTB robot simulation plug-in. Then the data in that motion state can be used as the standard to solve the motion state of the finger exoskeleton when making that motion in reverse.

4.2 Solidworks Model Results

The kinematics of the exoskeleton of the index finger is obtained by pre-setting the motion plan of the index finger in Solidworks according to the data in Fig.6 and performing the analysis of the motion algorithm.

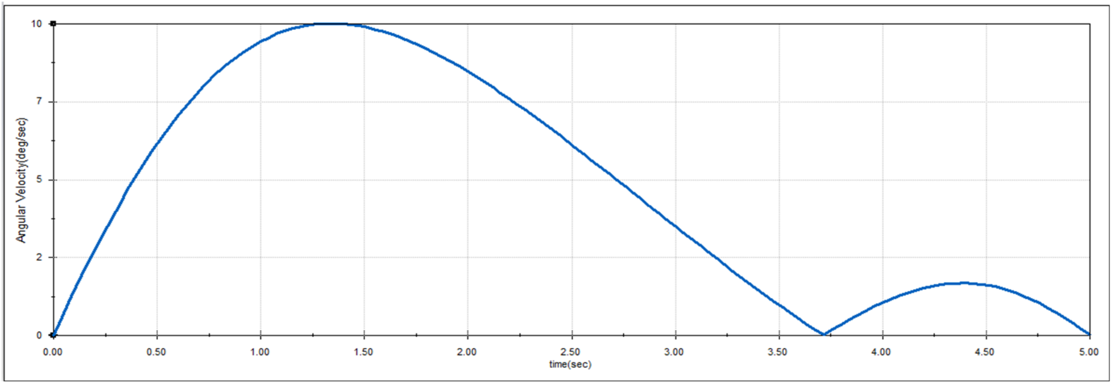

Fig 7. Angular velocity-time image of joint B (defined action time 5sec)

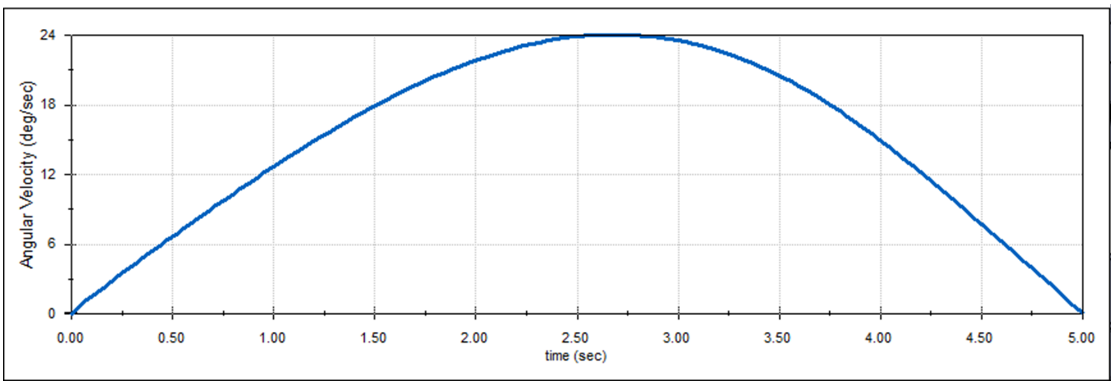

Fig 8. Angular velocity-time diagram of joint H

During the actuation of the exoskeleton, the relationship between the angular acceleration β of the exoskeleton driving joint and the driving moment M is:

$$M = J \cdot \beta$$

where J is the rotational moment of inertia. Therefore, the angular acceleration of the driven joint can be found to obtain the required driving torque of the joint. This gives an idea of the required power to be supplied by the driven Bowden cable.

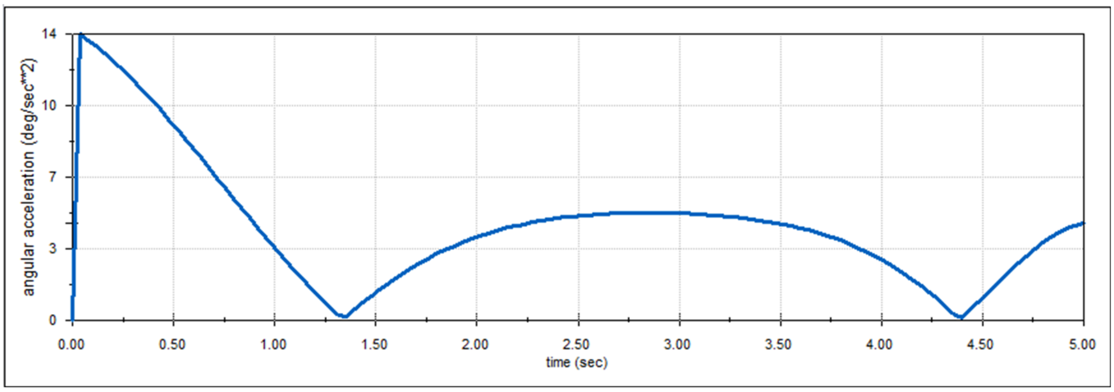

Fig 9. Angular acceleration-time diagram of joint B

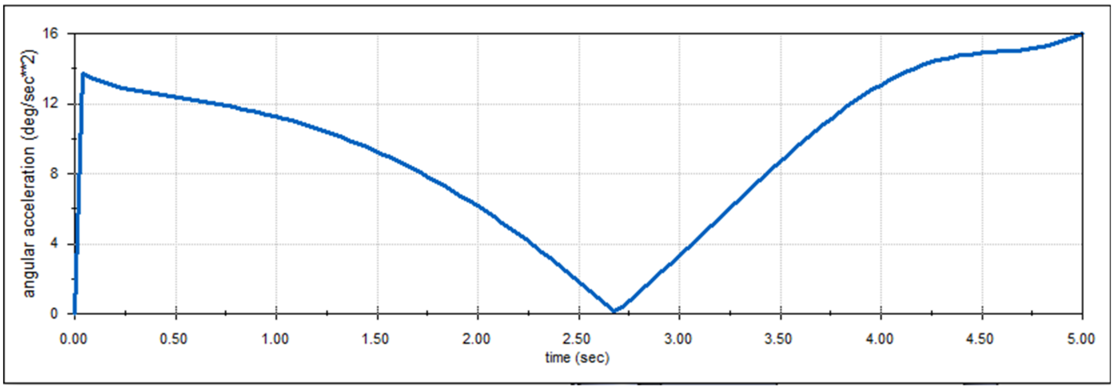

Fig 10. Angular acceleration-time diagram of joint H

In addition, the exoskeleton system has a prismatic pair, the composite hinge C, in its location. For the system to function properly, the displacement of the structure relative to the MCP joint should be the distance moved on the adjustable slider.

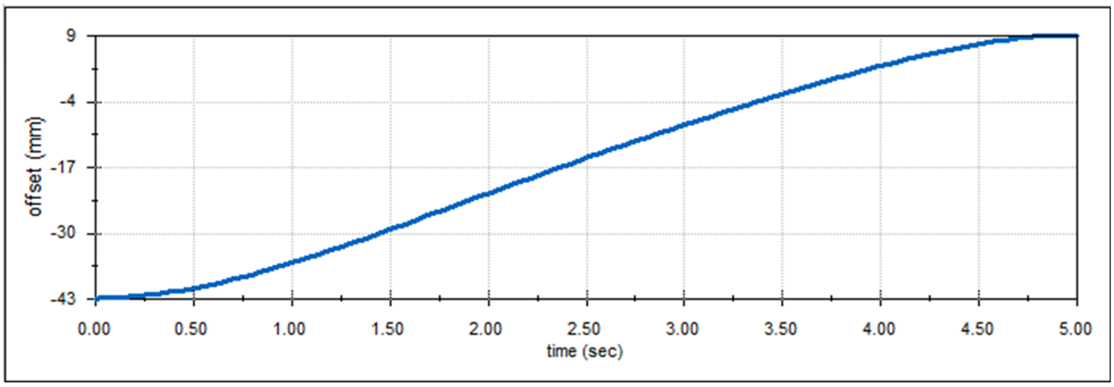

Fig 11. Displacement of joint C relative to MCP

5. Conclusion

This paper proposes and verifies an underactuated exoskeleton with higher adaptability and flexibility through design, theoretical calculation and modeling simulation. This work added sensors at two key points to improve the accuracy of data collection to ensure that the motion of the exoskeleton matches the motion characteristics of the wearer. This work also analyzed the kinematic relationship of the joint by formula derivation and calculation. At the same time, this work used modeling to simulate the angular acceleration of each node and the degree of displacement relative to MCP. Thus, the design and motion improvements this work has made makes the underactuated exoskeleton better suited to the rehabilitation needs of patients.

In addition, the skeleton has higher flexibility and adaptability than other exoskeletons, which greatly improves the recovery effect and reduces the production adaptation cost. However, the lack of clinical testing of actual finished products is one of the problems that need to be improved. In addition, this work intends in the future to develop a corresponding algorithmic program to fit the additional skeleton to provide the same degree of accuracy in the process of adjusting the different hand forms. This work also has a developing interest in how to improve structural strength and reduce wear and tear, and consider enhancing practicality while ensuring usability.

References

[1] He Yao. Population aging and healthy aging strategies in China[J]. China Chronic Disease Prevention and Control, 2012, 20(5): 507-509.

[2] Wang Lujing, Li Xianglei, Xu Dongqing. Characteristics and mechanisms of decreased hand fine motor ability in the elderly[J]. Chinese Journal of Rehabilitation Medicine, 2021.

[3] Wang C, Zhao D, Wu Guixian, et al. Trend analysis of stroke incidence in Beijing from 1984 to 1999[J]. Chinese Journal of Epidemiology, 2001, 22(4): 269-272.

[4] Neurological Rehabilitation Group of the Chinese Medical Association, Cerebrovascular Disease Group of the Chinese Medical Association, Stroke Screening and Prevention Project Committee Office of the Ministry of Health, et al. Chinese stroke rehabilitation treatment guidelines (2011 full version) [J]. Chinese Journal of Frontiers in Medicine, 2012, 4(6): 55-76.

[5] Evans RC. Illustrated Orthopedic Physical Assessment. Edinburgh: Mosby 2008.

[6] P. K. Levangie and C. C. Norkin. Joint Structure and Function: A Comprehensive Analysis, FA Davis, 2011.

[7] G. Zeng and A. Hemami, "An overview of robot force control," Robotica. 1997, 15(5), 473–482.

[8] L. L. Cai, A. J. Fong, C. K. Otoshi, Y. Liang, J. W. Burdick, R. R. Roy and V. R. Edgerton, "Implications of assist-as-needed robotic step training after a complete spinal cord injury on intrinsic strategies of motor learning," J. Neurosci. 2006, 26(41), 10564–10568.

[9] Priyanshu A, Youngmok Y, et al. "An index fifinger exoskeleton with series elastic actuation for rehabilitation: Design, control and performance characterization" in The International Journal of Robotics Research (2015).

[10] Zhou J, Malric F and Shirmohammadi S. A new hand measurement method to simplify calibration in cyberglovebased virtual rehabilitation. IEEE Transactions on Instrumentation and Measurement. 2010, 59(10): 2496–2504.

[11] Agarwal P, Yun Y, Fox J, et al. Design, control, and testing of a thumb exoskeleton with series elastic actuation[J]. The International Journal of Robotics Research, 2017, 36(3): 355-375.

[12] Yan Guangbin. Joint mobility (Range of motion, ROM) [J]. Chinese Journal of Joint Surgery: Electronic Edition, 2014, 8(3): 15-15.

[13] J. J. Craig. Introduction to Robotics: Mechanics and Control (vol. 3. Pearson/Prentice Hall, Upper Saddle River, NJ, USA), 2005.

[14] Deshpande AD, Gialias N and Matsuoka Y. Contributions of intrinsic visco-elastic torques during planar index finger and wrist movements. IEEE Transactions on Biomedical Engineering. 2012, 59(2): 586–594.

[15] Li Yong. Structural design and control research of finger rehabilitation training robot. Chongqing University of Technology, MA thesis, 2022.